DECEMBER 08 2004

Modifications of acoustic modes and coupling due to a leaning wall in a rectangular cavity

Y. Y. Li; L. Cheng

J. Acoust. Soc. Am. 116, 3312–3318 (2004)
https://doi.org/10.1121/1.1823331

Modifications of acoustic modes and coupling due to a leaning wall in a rectangular cavity

Y. Y. Li and L. Cheng[a)]
Department of Mechanical Engineering, The Hong Kong Polytechnic University, Hung Hom, Kowloon, Hong Kong SAR, China

(Received 1 January 2004; revised 24 September 2004; accepted 30 September 2004)

Acoustic modes and the coupling characteristics of a rectangular-like cavity with a slight geometrical distortion introduced through a leaning wall are investigated in this paper. A pressure variation index is proposed to quantify the global changes in acoustic modes caused by the inclination of the wall. Effects on the coupling between acoustic modes and structural modes are investigated using coupling coefficients. Numerical results show a simple relationship between the distortion effect and the acoustic wavelength. The effect is most significant when the distortion approaches the half wavelength. Compared with a rectangular enclosure, the existence of the leaning wall gives rise to a much more effective coupling between the structure and the enclosure. © *2004 Acoustical Society of America.* [DOI: 10.1121/1.1823331]

PACS numbers: 43.20.Ks, 43.20.Tb [MO] Pages: 3312–3318

I. INTRODUCTION

The study of sound radiation by a vibrating structure into an enclosure has received a great deal of attention for years. A comprehensive modal-based theoretical framework for interior sound field simulation was developed in the early work of Dowell *et al.*[1] and Fahy.[2] Since then, a large amount of effort has been devoted to investigating the vibro-acoustic behavior of such systems,[3,4] Given an excitation on the structure, structural vibration radiates sound into the enclosure through its coupling with acoustic modes. Therefore an accurate characterization of the sound-structure interaction plays a key role in the prediction of acoustic field. The interplay between the structure and the enclosure is usually characterized by the structural-acoustic modal coupling coefficient, which is a measure of the spatial match between structure modes and cavity modes. The coupling analysis can be easily done for cavities with simple geometry,[5,6] due to the existence of analytical modal solutions.[7] This exercise turns out to be very useful in many aspects,[8,9] especially in revealing useful physical insights to lead subsequent sound control strategies.[10–13]

Literature review shows that most of previous work dealt with rectangular or cylindrical enclosure. Although the use of such regular-shaped cavities with perfect geometry greatly simplifies the modeling procedure, one of the direct consequences of such assumption is that, due to the symmetry in both the structure and the enclosure, the structural-acoustic coupling occurs in a very selective way, which physically means that a structure mode can only be coupled to a small portion of acoustic modes to warrant an effective sound radiation.[10,12] In practice, however, slight imperfection in geometry always exists, which may affect the acoustic mode shapes and, consequently, bring drastic changes in the coupling nature. As a first step, it is necessary to comprehend how acoustic modes are altered. Literature survey shows that few works on the irregular-shaped cavity have been reported. One of the plausible reasons is that, classical modal-based methods rely on the availability of acoustic modes, which cannot be analytically known in the presence of geometry irregularity. For a long time, numerical methods, such as the finite element method[14] and the boundary element method,[15] have been adopted to deal with the problem. The development of acoustoelastic method[16] and the Green function method[17] made it possible to handle the irregular shaped cavities in a semi-analytical way. Both methods were then improved by the authors, who proposed the ''combined integro-modal (CIM) approach,'' in which the cavity was discretized into a series of subcavities, and the acoustic pressure was decomposed either over a modal basis of regular subcavities or over that of the bounding cavities in the case of irregular-shaped boundaries.[18,19] Comparisons between theoretical or other existing results and the presented numerical solutions showed excellent agreement.[20]

The purpose of this paper is to investigate possible changes in acoustic modes and coupling characteristics due to the introduction of a leaning wall in a rectangular-like cavity. The whole system is modeled using the CIM approach. A pressure variation index is defined to quantify the global change in acoustic modes caused by the wall inclination. The tendency plots of index reveal the relationship between the distortion effect and the wavelength of acoustic modes involved. The impact on the structural-acoustic coupling is also examined.

II. FORMULATION

As shown in Fig. 1, the cavity under investigation is a rectangular-like cavity with one leaning wall (a trapezoidal enclosure). The enclosure has a volume V_0 (cavity with solid lines) surrounded by a surface S_0 which is acoustically rigid. A small angle α, which defines the degree of the inclination of the leaning wall S_1, is used to represent the geometry

a)Author to whom correspondence should be addressed; electronic address: mmlcheng@polyu.edu.hk

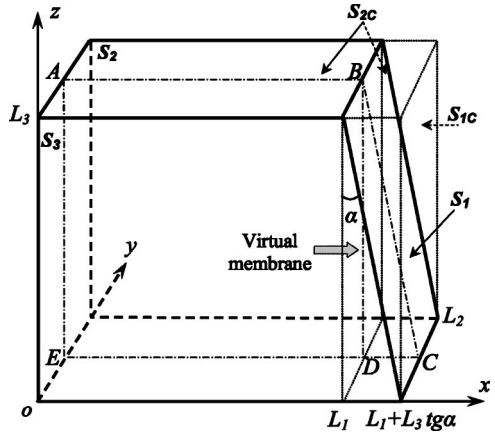

FIG. 1. Geometry and coordinate system of a rectangularlike cavity with one leaning wall.

distortion of the cavity, as opposed to its rectangular counterpart. The acoustic pressure Ψ inside the enclosure can be expressed in the form of wave equation

$$(\nabla^2+k^2)\Psi=0 \tag{1}$$

with the Neumann boundary condition

$$(\partial\Psi/\partial\mathbf{n})_{S_0}=0, \tag{2}$$

where k is the wave number and $\mathbf{n}$ the normal direction towards outside. In parallel, a rectangular bounding cavity, which encloses the trapezoidal enclosure V_0 and occupies a volume V_c $((L_1+L_3\times tg\alpha)\times L_2\times L_3)$ with a surface S_c, is constructed (dashed in Fig. 1). Inside the bounding cavity, the Green's function $G(r,r_0)$ satisfies the following inhomogeneous Helmholtz equation with a point source:

$$(\nabla^2+K^2)G(r,r_0)=-\delta(r-r_0), \tag{3a}$$

$$(\partial G(r,r_0)/\partial\mathbf{n})_{S_C}=0, \tag{3b}$$

where $\delta(r-r_0)$ is the Dirac delta function. $G(r,r_0)$ can be expressed in terms of normal modes φ_p of the bounding cavity V_c as

$$G(r,r_0)=\sum_{l,m,n}\frac{\varphi_{lmn}(r)\varphi_{lmn}(r_0)}{(k_{lmn}^2-k^2)V_R\wedge_{lmn}}, \tag{4}$$

where

$$\varphi_{lmn}=\cos\left(\frac{l\pi x}{L_1+L_3\cdot tg\alpha}\right)\cos\left(\frac{m\pi y}{L_2}\right)\cos\left(\frac{n\pi z}{L_3}\right), \tag{5a}$$

with k_{lmn} and $\wedge_{lmn}$ being, respectively, the wave number and the generalized acoustic mass of the lmn-th mode, viz.

$$k_{lmn}^2=\left(\frac{l\pi}{L_1+L_3\cdot tg\alpha}\right)^2+\left(\frac{m\pi}{L_2}\right)^2+\left(\frac{n\pi}{L_3}\right)^2, \tag{5b}$$

$$\wedge_{lmn}=\frac{1}{V_c}\int_{V_c}\varphi_{lmn}(r)\varphi_{lmn}(r)dv. \tag{5c}$$

According to the CIM approach,[18,20] the acoustic pressure inside V_0 is decomposed on the basis of normal modes φ_{lmn} of the bounding cavity as

$$\Psi=\sum_{l,m,n}b_{lmn}\varphi_{lmn},\quad l=1,...,L;\quad m=1,...,M;\quad n=1,...N, \tag{6}$$

where b_{lmn} are the unknown coefficients to be determined; (L,M,N) the numbers of the terms to be kept after the truncation of the series. Combining Eqs. (1)–(4) with (6) and using the orthogonality property of mode shapes lead to the following eigenvalue equation:

$$(k^2-k_{lmn}^2)b_{lmn}=\sum_{i,j,k}b_{ijk}n_{lmn,ijk}(\alpha), \tag{7}$$

where

$$n_{lmn,ijk}(\alpha)=\int\int_{S_0}\varphi_{ijk}\frac{\partial\varphi_{lmn}}{\partial\mathbf{n}}ds. \tag{8}$$

For the cavity V_0, $\partial\varphi_{lmn}/\partial\mathbf{n}=0$ holds at all walls except on the leaning wall S_1. In light of the relationship between variables x and z:

$$x=L_1+(L_3-z)\cdot tg\alpha, \tag{9}$$

one has

$$\frac{\partial\varphi_{lmn}}{\partial\mathbf{n}}=-\cos\frac{m\pi y}{L_2}\left(\frac{l\pi\cos\alpha}{L_1+L_3tg\alpha}\times\sin\frac{l\pi x}{L_1+L_3tg\alpha}\cos\frac{n\pi z}{L_3}+\frac{n\pi\sin\alpha}{L_3}\cos\frac{l\pi x}{L_1+L_3tg\alpha}\sin\frac{n\pi z}{L_3}\right). \tag{10}$$

Substituting Eq. (10) into (8) and then integrating over S_1, $n_{lmn,ijk}(\alpha)$ can be expressed as

$$n_{lmn,ijk}(\alpha)=\frac{[1-|\mathrm{sign}(m-j)|]\pi L_2}{16}\cdot\left\{\frac{l\cos\alpha}{L_1+L_3tg\alpha}[c_1(a_1-a_2+a_3-a_4)+|\mathrm{sign}(l-i)|\cdot c_2(a_5-a_6+a_7-a_8)]+\frac{n\sin\alpha}{L_3}[c_1(a_1+a_2+a_3+a_4)+c_2(a_5+a_6+a_7+a_8)]\right\}, \tag{11}$$

where $(c_1, c_2, a_1, ..., a_8)$ are a set of coefficients which can be calculated for a given α. sign is a symbol function defined as

$$\mathrm{sign}(x)=\begin{cases}1, & x>0\\ 0, & x=0\\ -1, & x<0\end{cases}.$$

It is clear that $n_{lmn,ijk}(\alpha)$ vanishes when $\alpha=0$, showing the orthogonality property of the modes when there is no distortion. Rearranging Eq. (7) in the matrix form gives

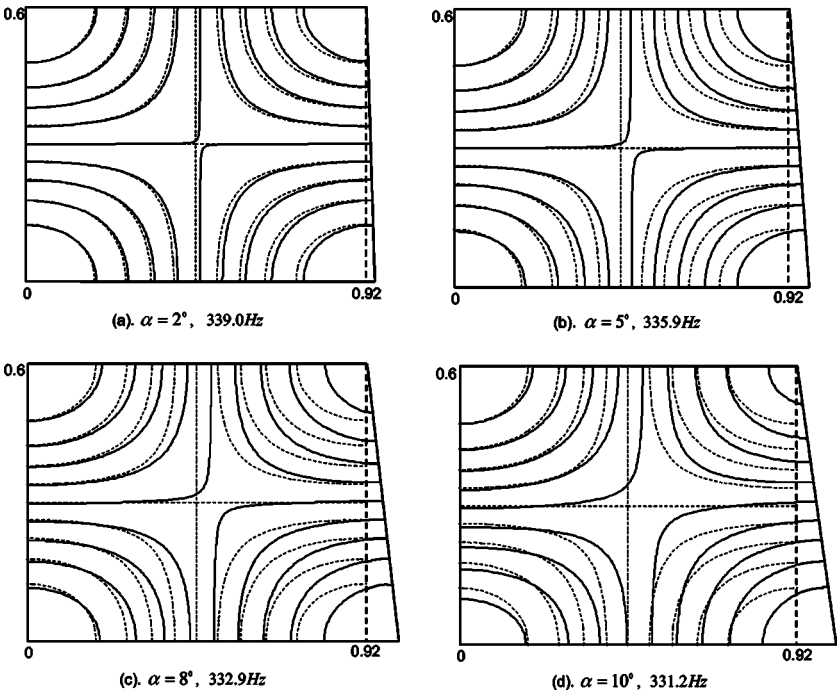

FIG. 2. Contour of the iso-pressure of the acoustic mode (1,0,1) over the cross area $ABCE$.

$$\begin{bmatrix} n_{000,000}(\alpha)-(k^2-k_{000}^2) & \cdots & n_{000,LMN}(\alpha) \\ \cdots & \cdots & \cdots \\ n_{LMN,000}(\alpha) & \cdots & n_{LMN,LMN}(\alpha)-(k^2-k_{LMN}^2) \end{bmatrix} \begin{Bmatrix} b_{000} \\ \vdots \\ b_{LMN} \end{Bmatrix} = \mathbf{0}. \tag{12}$$

The solution of Eq. (12) yields b_{lmn} for constructing acoustic pressure (or acoustic mode shape) inside the cavity from Eq. (6).

In order to quantify changes in acoustic modes, a variation index is defined as

$$J_{lmn}(\alpha) = \int_S \Delta\Psi_{lmn}^2(\alpha)ds, \tag{13}$$

where $\Delta\Psi_{lmn}(\alpha)$ is the residual mode shape over a given surface S:

$$\Delta\Psi_{lmn}(\alpha) = \Psi_{lmn}(\alpha) - \Psi_{lmn}(\alpha=0). \tag{14a,b}$$

Obviously, $J_{lmn}(\alpha)$ represents the global change in the lmn-th mode over the surface caused by the wall inclination.

III. NUMERICAL SIMULATION AND DISCUSSIONS

The formulation described in Sec. II is implemented. The dimension of the cavity is set as $L_1 \times L_2 \times L_3 = 0.92 \times 0.15 \times 0.6$ m^3. Since the inclination is introduced parallel to y-axis, discussions will focus on those modes with order (l,m,n) with $m=0$. In the following discussions, the term "(l,m,n) mode" will be used to designate a pair of acoustic modes before and after α is introduced. It should be mentioned that although this notation has clear physical meaning when $\alpha=0$, it is loosely used for the cavity with a leaning wall for the sake of convenience. In the latter case, it simply stands for a mode evolving from the (l,m,n) mode ($\alpha=0$) due to the wall inclination. The matching of the pair is ensured by carefully checking the mode shape (pressure distribution) of each mode during the calculation.

The truncation of the decomposition series [Eq. (6)] is a main factor affecting the accuracy of the calculation. A careful convergence analysis was carried out by following the procedure detailed in our previous work.[18] Roughly speaking, (L,M,N) was gradually increased until no noticeable changes in the calculated results were observed. For the present configuration, the series is truncated up to 60, 3, and 10 in L, M, and N, respectively.

A. Analysis of acoustic modes

Changes in acoustic pressure distribution due to the variation of α are first investigated by choosing one typical mode (1,0,1). Figure 2 shows the contour plot of the acoustic pressure over the cross area $ABCE$ ($y=L_2/2$ in Fig. 1) with different inclination angles. The dashed are the iso-pressure lines when $\alpha=0°$ taken as the nominal case. The pressure amplitude is normalized to the maximal pressure value in the cavity. It can be seen that the distortion has no significant influence on natural frequencies, due to the large wavelength of the mode with respect to the distortion. With the increase of α from 2° to 10°, the mode shape deviates gradually from its nominal case. This change in acoustic pressure is quantified by the residual mode shape $\Delta\Psi_{101}(\alpha)$ in Fig. 3. It can be seen that:

- For the case of $\alpha=2°$, change in the acoustic mode is observed, and the maximal difference is 4% compared to

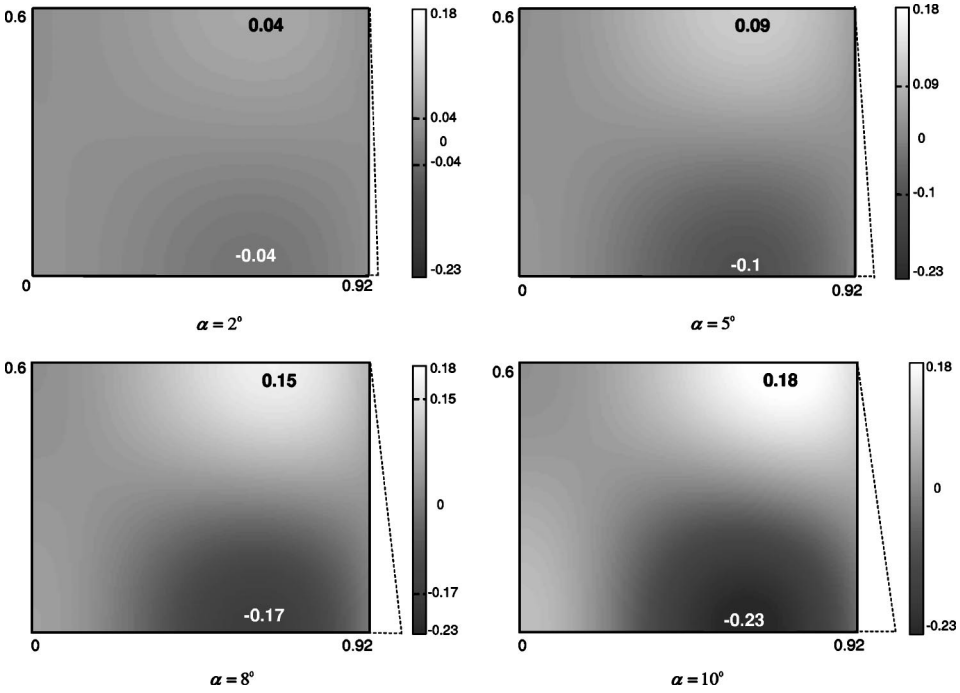

FIG. 3. Residual acoustic pressure $\Delta\Psi_{101}(\alpha)$.

the nominal one. With the increase of α, this change becomes more significant, reaching 23% for $\alpha=10°$.

- The perfect symmetry of mode shape at edges AB and DE in the case of $\alpha=0°$ is altered due to the distortion.
- There is a maximum pressure change area at edge AB for each configuration, ranging from 0.04 to 0.18. Its location gradually moves towards the leaning wall of the enclosure when α increases. For the same token, an even larger variation area (from 0.04 to 0.23) can be observed at the bottom part of the cavity (edge DE), with the same moving tendency as shown at edge AB. In comparison, there is little change on the surface opposite to the leaning wall. Therefore, the effect of α on acoustic pressure variation is mainly on the two walls adjacent to the inclined wall rather than on the opposite one, with the maximal variation appearing at the area close to the leaning wall.

The global variation of a number of selected acoustic modes is quantified using the variation index $J_{lmn}(\alpha)$. Figure 4 illustrates the tendency curve of $J_{l00}(\alpha)$ for a number of selected modes with α varying from 0° to 30°. It can be seen that

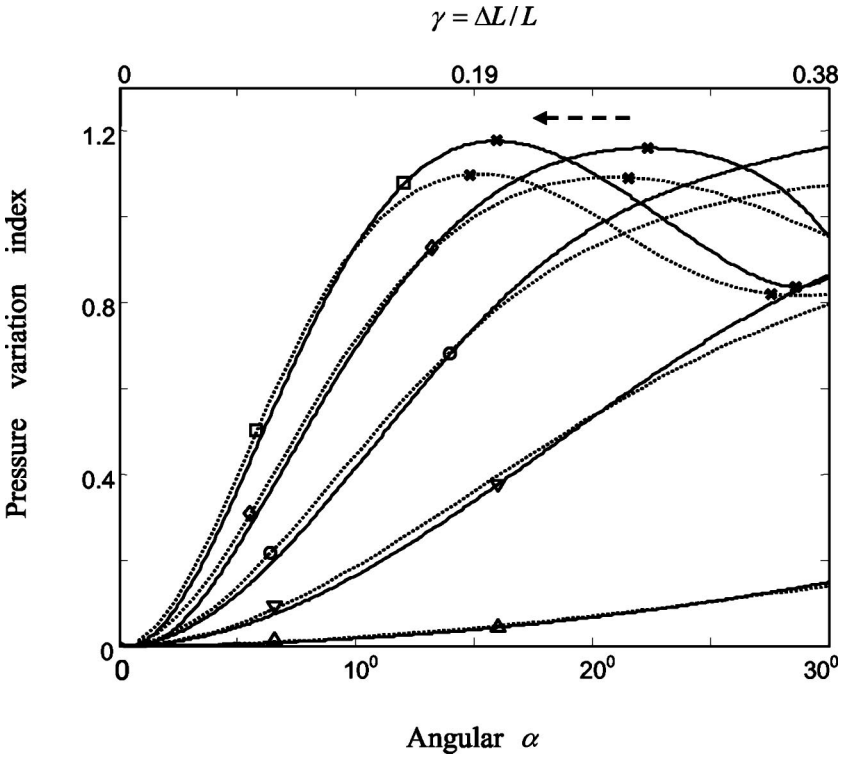

FIG. 4. Pressure variation index. Solid line: acoustic modes (l, 0,0) with $0° \leqslant \alpha \leqslant 30°$ at S_2; dashed: 1D duct modes with γ varying from 0 to 0.38. △: $l=1$; ▽: $l=3$; ○: $l=5$; ◇: $l=7$; □: $l=9$.

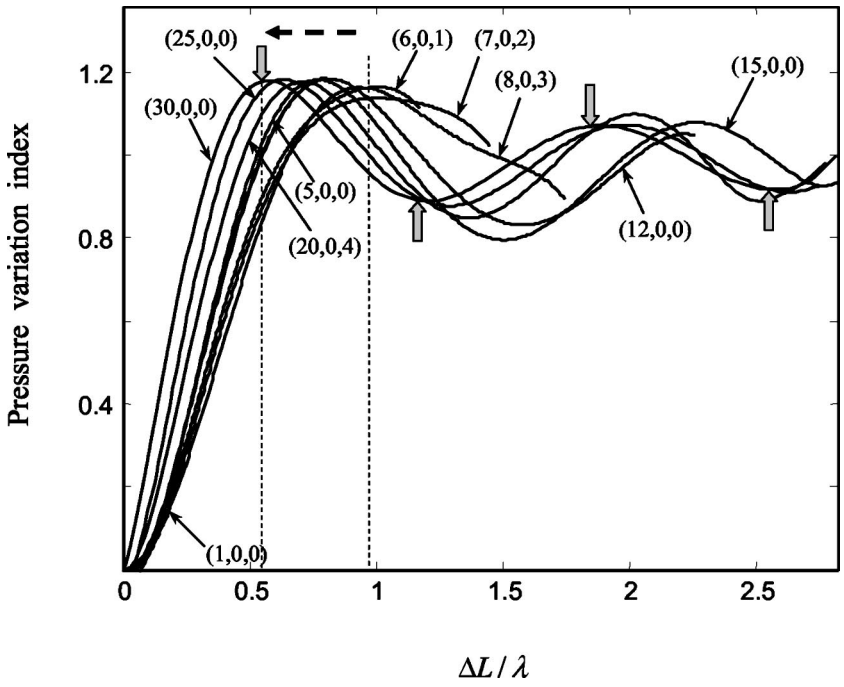

FIG. 5. Pressure variation index $J_{lmn}(\alpha)$ at S_2 vs $\Delta L/\lambda$ with $0° \leqslant \alpha \leqslant 30°$ ($\Delta L = L_3 \cdot tg\,\alpha, L_3 = 0.6$).

- For a small α, the variation index $J_{l00}(\alpha)$ increases with the increase of order l. That is, a certain distortion will have a more sensitive effect on pressure variation for high-order modes than for low-order ones.
- Within the range of interest, no extremum of $J_{l00}(\alpha)$ is observed for low-order modes. However, peaks appear with the increase of l. For example, $J_{l00}(\alpha)$ reaches its maximum at $\alpha \approx 22°$ for mode (7,0,0) and at $\alpha \approx 16°$ for mode (9,0,0). With further increase of l, multiple peaks emerge.

The earlier results show that there are critical values of α for each mode in which the variation is the most remarkable. There might be a relationship between these critical values and the wavelength of modes in question. Quantifying this possible relationship can help estimate the impact of distortion on one particular mode of interest.

Since α mainly affects the acoustic modes in x-direction, an auxiliary study was performed using a one-dimensional (1D) duct with a length L to understand the observed phenomena. Some details are given in the Appendix. Using the duct theory,[21] it can be found that maximum alteration in the acoustic pressure occurs at those locations ΔL satisfying

$$\Delta L|_{i=l-1,l-2,\ldots} = \frac{\lambda l}{2}\left(\frac{l}{i}-1\right) = \left(\frac{l}{i}-1\right)L, \quad \lambda = \frac{2L}{l}, \quad (15)$$

and the *first* one is located at

$$\Delta L|_{i=l-1} = \frac{\lambda}{2}\cdot\frac{l}{l-1}. \quad (16)$$

Clearly, the number and locations of extrema depend on the wavelength λ and mode order l. For the *first* one, an increase in l makes $\Delta L/\lambda$ approaching 0.5, implying that for high-order modes, the change in acoustic modes is the most remarkable when $\Delta L \to \lambda/2$. Since higher-order modes have shorter wavelength, a slight distortion can therefore lead to a significant variation of mode shapes. Results are also plotted in Fig. 4 and compared with previous ones for the cavity, showing a strong similarity.

This observation is further verified in Fig. 5 using the cavity defined before, which illustrates the variation of $J_{lmn}(\alpha)$ ($0° \leqslant \alpha \leqslant 30°$) with respect to $\Delta L/\lambda$ ($\Delta L = L_3 \cdot tg\,\alpha$). A large variety of modes are included in the figure to check the observation made earlier. It should be mentioned that, due to the difference in wavelength of different modes, the variation ranges of $\Delta L/\lambda$ are not the same for all modes considered. The highest mode involved is 30 in x-direction of the cavity, for which *four* extremum are detected at $\Delta L/\lambda = 0.55$, 1.15, 1.8, and 2.54, respectively (marked with arrows in the figure). This result is in consistent with the prediction given by Eq. (15), which are $\Delta L/\lambda|_{i=29,\ldots,26} = 0.52$, 1.07, 1.67, and 2.3. In addition, with the increase of mode order l, the *first* extremum $\Delta L/\lambda|_{i=l-1}$ indeed convergences to 0.5.

The effect of the inclination on different walls is also examined. Two walls, i.e., S_2 which is adjacent to the leaning wall and S_3 which is opposite to it are taken as example, and the pressure variation indices for a number of selected modes are compared in Fig. 6. Apparently, the distortion has much greater effect on S_2 than S_3.

B. Vibroacoustic coupling analysis

Replacing the top wall of the enclosure by a simply-supported flexible panel, a coupling analysis is conducted to quantify the effects of the wall inclination on the structural-acoustic coupling feature. The commonly used coupling coefficient $L(\alpha)$ is defined as the integral of the product between ij-th structure mode ϕ_{ij} and the lmn-th cavity mode $\Psi_{lmn}(\alpha)$ over the vibrating surface A_f:

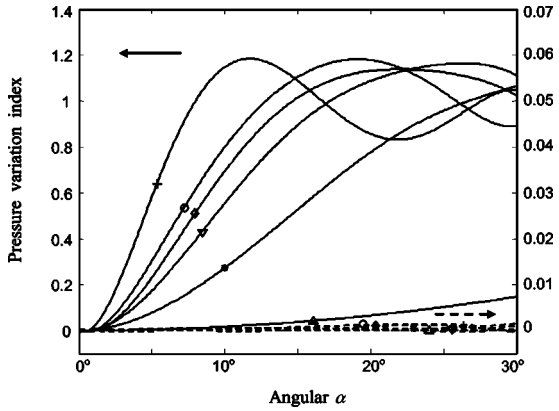

FIG. 6. Pressure variation index $J_{lmn}(\alpha)$ with $0° \leqslant \alpha \leqslant 30°$ at S_2 (solid line) and S_3 (dashed). △:(1,0,0); *: (4,1,2); ▽: (6,0,1); ◇: (7,0,2); ○: (8,0,2); +: (12,0,0).

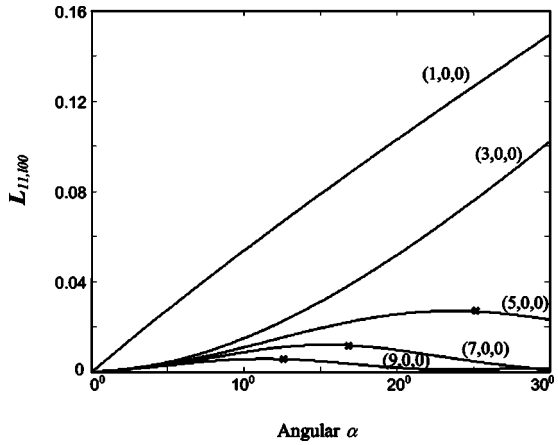

FIG. 8. Effect of α on the coupling coefficient $L_{11,l00}$ ($l=1,3,...,9$).

$$L_{ij,lmn}(\alpha) = \frac{1}{A_f} \int \phi_{ij} \Psi_{lmn}(\alpha) ds. \tag{17}$$

Figure 7 compares the magnitude of the coupling coefficients when $\alpha=0$ and $\alpha=10°$ using sixteen acoustic modes ($l=0,...,3; m,n=0,1$) and nine structural modes ($i,j=1,..,3$). It can be seen that, when $\alpha=0$, only a few acoustic modes are coupled to each structural mode (denoted by a star in Fig. 7). In fact, any symmetric/anti-symmetric modes of the panel, with respect to the center, would not be coupled to an acoustic mode if the latter is anti-symmetrical/symmetrical in one of the two directions parallel to the panel surface. The distortion of the wall ($\alpha=10°$) greatly increases the number of the coupled modes, denoted by circles in Fig. 7. Comparing the two cases, the coupling strength between the originally coupled modes are not significantly altered, as judged by the closeness of the star-circle pairs in Fig. 7. The additional coupling caused by the inclination of the wall, however, can reach a relatively high level in some cases. For example, $L_{31,300}(0)=0$ between the (3,1) mode and the (3,0,0) mode while $L_{31,300}(10°)=0.15$ (marked with an arrow in the figure), attaining 37% of the maximum values of $L_{ij,lmn}(\alpha)$ ($L_{11,100}(\alpha)=0.4053$). Apparently, a strong coupling is created due to the distortion of the enclosure.

Taking the structural mode (1,1) as an example, variations of the coupling strength with respect to α are examined in Fig. 8. The *five* acoustic modes are the same as the ones previously used in Fig. 4. For each particular acoustic mode, the general tendency of the curve is somehow similar to its counterpart in Fig. 4, which implies that a maximum alteration of the pressure would most likely also lead to a significant change in its coupling strength to the lower-order structural modes. This agreement becomes, however, less consistent, for higher-order structural modes (not shown). Therefore, the criterion previously established to quantify the pressure variation can be roughly used to predict the coupling strength between an acoustic mode with a lower-order structural mode.

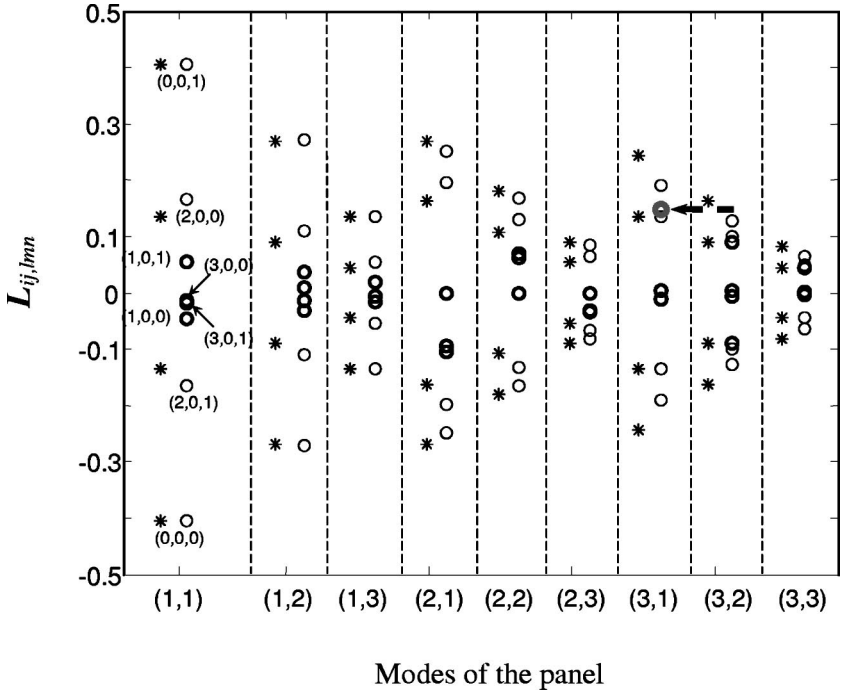

FIG. 7. Coupling coefficient $L_{ij,lmn}$ between acoustic modes and structural modes of a simply-supported panel. *: $\alpha=0$ and ○: $\alpha=10°$ ($i,j=1,...,3$; $l=0,...,3$; $m,n=0,1$).

IV. CONCLUSIONS

Acoustic modes and the coupling characteristics of a rectangular-like cavity with a slight geometrical distortion introduced through a leaning wall are investigated in this paper. A pressure variation index is proposed to quantify the global change in acoustic modes. The coupling coefficient is used to measure the effect caused by the distortion. Numerical simulations are performed to find out the relationships between the variation index, the coupling coefficient and the distortion. The following conclusions can be drawn.

(1) The pressure distribution inside the cavity is sensitive to geometrical changes. The most affected areas move to the leaning wall when the distortion is getting larger.

(2) A simple relationship between the distortion effect and the acoustic wavelength involved is established. Whether a given distortion is important depends on the wavelength of the acoustic modes. For a lower-order mode, a small distortion has no apparent influence due to its large acoustic wavelength. For high-order modes, however, the effect is apparent and intensifies when the distortion approaches the half wavelength.

(3) The distortion affects more the two adjacent walls than the opposite one.

(4) The inclination of the wall gives rise to a much more effective coupling between the structure and the enclosure. The most affected modes are these pairs which are not initially coupled when $\alpha=0$. The coupling strength between an acoustic mode and a lower-order structural mode roughly follows the tenancy stated in (2).

ACKNOWLEDGMENTS

This project was supported by the Hong Kong Polytechnic University Research Grant No. (G-U031) and the Research Grants Committee of HKSAR (Grant No. PolyU 5165/02E).

APPENDIX: RELATIONSHIP BETWEEN THE DISTORTION AND THE WAVELENGTH OF A ONE-DIMENSIONAL DUCT

The l-th mode shape of a duct with a length L satisfies $\Psi_l=\cos(l\pi x/L)$, and the corresponding residual mode shape when the length varies from L to $L(1+\gamma)$ can be written as

$$\Delta\Psi_l(\gamma)=\cos\left(\frac{l\pi x}{L(1+\gamma)}\right)-\cos\left(\frac{l\pi x}{L}\right),\quad \gamma=\frac{\Delta L}{L}. \tag{A1}$$

Using the pressure variation index defined in Eq. (13):

$$\begin{aligned}J_l(\varepsilon)&=\int_0^L \Delta\Psi_l^2(\varepsilon)dx\\&=L\left(1+\frac{\sin(2\pi l\varepsilon)}{4\pi l\varepsilon}+\frac{1}{l\pi}\left(\frac{(-1)^{l+1}}{1+\varepsilon}+\frac{(-1)^l}{1-\varepsilon}\right)\sin(l\pi\varepsilon)\right),\\ \varepsilon&=\frac{1}{1+\gamma}.\end{aligned} \tag{A2}$$

$J_l(\varepsilon)$ reaches its extrema when $\partial J_l(\varepsilon)/\partial\varepsilon=0$, i.e.:

$$\begin{aligned}&\frac{1}{4\varepsilon^2}\sqrt{1+(2\pi l\varepsilon)^2}\sin(\operatorname{arctg}(2\pi l\varepsilon)-2\pi l\varepsilon)\\&\quad+\frac{2}{1-\varepsilon^2}\sqrt{\left(\frac{1+\varepsilon^2}{1-\varepsilon^2}\right)^2+(\pi l\varepsilon)^2}\sin\left(l\pi\varepsilon+\operatorname{arctg}\frac{l\pi\varepsilon(1-\varepsilon^2)}{1+\varepsilon^2}\right)=0.\end{aligned} \tag{A3}$$

A simplification of Eq. (A3) results in an approximate solution of ε, viz., $\varepsilon=i/l$ $(i=1,...,n)$. Thus, one has

$$\Delta L|_{i=l-1,l-2,...}=\frac{\left(\frac{l}{i}-1\right)\lambda l}{2}=\left(\frac{l}{i}-1\right)L. \tag{A4}$$

where λ is the wavelength of the l-th mode and $\lambda=2L/l$.

[1] E. H. Dowell, G. F. Gorman, and D. A. Smith, "Acoustoelasticity: General theory, acoustic natural modes and forced response to sinusoidal excitation, including comparisons with experiment," J. Sound Vib. **52**, 519–541 (1977).
[2] F. J. Fahy, *Sound and Structural Vibration* (Academic, England, 1987).
[3] J. Pan, "Analysis of low frequency acoustic response in a damped rectangular enclosure," J. Sound Vib. **223**, 543–566 (1999).
[4] J. H. Wu, H. L. Chen, and W. B. An, "A method to predict sound radiation from a plate-ended cylindrical shell excited by an external force," J. Sound Vib. **237**, 793–803 (2000).
[5] L. P Franzoni and D. B. Bliss, "A discussion of modal uncoupling and an approximate closed-form solution for wealy-coupled systems with application to acoustics," J. Acoust. Soc. Am. **103**, 1923–1932 (1998).
[6] K. S. Sum and J. Pan, "On acoustic and structural modal cross-couplings in plate-cavity systems," J. Acoust. Soc. Am. **107**, 2021–2038 (2000).
[7] P. M. Morse and K. U. Ingard, *Theoretical Acoustics* (McGraw-Hill, New York, 1968).
[8] R. F. Keltie and H. Peng, "The effects of modal coupling on the acoustic power radiation from panels," J. Vibr. Acoust. **109**, 48–54 (1987).
[9] K. A. Cunefare, "Effect of modal interaction on sound radiation from vibrating structures," AIAA J. **30**, 2819–2828 (1992).
[10] L. Cheng and J. Nicolas, "Radiation of sound into a cylindrical enclosure from a point-driven end plate with general boundary conditions," J. Acoust. Soc. Am. **91**, 1504–1513 (1992).
[11] L. F. Peretti and E. H. Dowell, "Asymptotic modal-analysis of a rectangular acoustic cavity excited by wall vibration," AIAA J. **30**, 1191–1198 (1992).
[12] J. Pan, "The forced response of an acoustic-structural coupled system," J. Acoust. Soc. Am. **91**, 949–956 (1992).
[13] M. Kronast and M. Hildebrandt, "Vibro-acoustic modal analysis of automobile body cavity noise," Sound Vib. **34**, 20–23 (2000).
[14] M. Petyt, J. Lea, and G. H. Koopman, "A finite element method for determining the acoustic modes of irregular shaped cavities," J. Sound Vib. **45**, 497–502 (1976).
[15] C. A. Brebbia, J. C. F. Telles, and L. C. Wrobel, *Boundary Element Techniques* (Springer, New York, 1984).
[16] C. F. Chao, E. H. Dowell, and D. B. Bliss, "Modal analysis of interior noise field," Vib. Conf. Design Eng. 1981.
[17] G. P. Succi, "The interior acoustic field of an automobile cabin," J. Acoust. Soc. Am. **81**, 1688–1694 (1987).
[18] J. Missaoui and L. Cheng, "A combined integro-modal approach for predicting acoustic properties of irregular-shaped cavities," J. Acoust. Soc. Am. **101**, 3313–3321 (1997).
[19] J. Missaoui and L. Cheng, "Vibroacoustic analysis of a finite cylindrical shell with internal floor partition," J. Sound Vib. **226**, 101–123 (1999).
[20] E. Anyunzoghe and L. Cheng, "Improved integro-modal approach with pressure distribution assessment and the use of overlapped cavities," Appl. Acoust. **63**, 1233–1255 (2002).
[21] P. M. Morse and M. Foshbach, *Methods of Theoretical Physics* (McGraw-Hill, New York, 1953)